THE PARTITION OF ENERGY INTO WAVES AND CURRENTS

W. Perrie, C. Tang, Y. Hu and B.M. DeTracy

Fisheries & Oceans Canada, Bedford Institute of Oceanography, Dartmouth, Nova Scotia , Canada

1. INTRODUCTION

Ocean models usually estimate surface currents without explicit modelling of the ocean waves. To consider the impact of waves on surface currents, we use a wave model in a modified Ekman layer model, which is imbedded in a diagnostic ocean model. Thus, we explicitly consider wave effects, for example Stokes drift and wave-breaking dissipation, in conjunction with the Ekman current, mean currents and wind-driven pressure gradient currents. This is an explicit implementation of the equations for wave-induced currents, as derived by Jenkins (1987ab). WAM-type model terms are used to estimate energy input to waves by wind and removed by wave-breaking dissipation. The ocean model follows that described by Tang et al. (1999). Previously these equations by Jenkins were used to estimate wave-induced forcing on ice floes (Perrie and Hu, 1997). This coupled wave-ocean model is compared to measurements from the Labrador Sea Deep Convection Experiment of 1997. We show that the wave effect is largest in rapidly developing intense storms, when wave-modified currents can briefly exceed the usual Ekman currents by as much as 40%. A large part of the increase in velocity can be attributed to the Stokes drift. Reductions in momentum transfer to the ocean due to wind input to waves, and enhancements due to wave breaking dissipation are each of the order 20-30%.

2. NUMERICAL MODEL

In the absence of waves, the near-surface currents can be obtained by solving the governing equations of the ocean model at the surface. If the model has sufficient vertical resolution, these equations include an Ekman layer. The presence of waves modifies the Ekman layer and the associated surface currents, resulting from wind inputs into waves, wave evolution and wave-breaking. To account for wave-induced currents, it is necessary to replace the ocean model's original Ekman layer with a wave-modified Ekman layer.

2.1 Wave Model

Ocean wave spectra usually considers three dominant processes: input of energy to the waves by wind, S_{in}, non-linear transfer between spectral components due to wave-wave interactions, S_{nl}, and dissipation due to white-capping and wave-breaking, S_{ds}, which transfers energy to currents. Three processes are described for the WAM operational wave model by Hasselmann et al. (1988) and Komen et al. (1994). The corresponding balance equation describing wave growth and development is

$$\frac{\partial E(t,x,f,\theta)}{\partial t} + \mathrm{C}_g \cdot \nabla E(t,x,f,\theta) = S_{in} + S_{ds} + S_{nl} \tag{1}$$

where $E(t,x,f,\theta)$ is the two-dimensional wave spectrum in terms of frequency f, wave propagation direction, θ, time, t, and position, x, and where C_g is the group velocity. In this study, we extend the approach of Jenkins (1987ab, 1989) and Perrie and Hu (1997) by coupling the wave model to a simple realistic three-dimensional ocean model (Tang and Gui, 1996). This allows us to estimate the impact of surface waves on surface currents. We do not consider other coupling mechanisms here, such as the impact of currents on waves.

3. Ocean Model

We assume that the density current in the Ekman layer is much smaller than the Ekman current. This is generally a valid assumption in the Labrador Sea and the Grand Banks, because wind mixing and winter cooling create a surface mixed layer of uniform density in the upper tens to hundreds of meters of the water column. We use a diagnostic ocean model in which the water density does not change with time. The governing equations are given by

$$\frac{\partial \mathrm{u}}{\partial t} + \mathbf{f} \times \mathrm{u} = -\frac{1}{\rho_o} \nabla p + \frac{\partial}{\partial z}(-\overline{w'\mathrm{u}'}) \tag{2}$$

$$\nabla \cdot \mathrm{u} + \frac{\partial w}{\partial z} = 0 \tag{3}$$

$$p = g\rho_o \zeta + g\int_z^0 \rho dz \tag{4}$$

where $\mathbf{f}$ is the Coriolis parameter and the (horizontal, vertical) components of velocity are $(\mathbf{u}, w)$, respectively. We assume co-ordinates where z is upward and ζ is the adjusted sea level. Water density is ρ and ρ_o is a reference density. The last term of Equation (2) is the vertical gradient of the Reynolds stress, which is created by wind-mixing and wave effects. This term is assumed significant only in the Ekman layer. The horizontal current is represented by a decomposition into an interior velocity, u_i, and an Ekman velocity, u_w:

$$\mathrm{u} = \mathrm{u}_i + \mathrm{u}_w . \tag{5}$$

The Ekman current u_w is large only in the Ekman layer. The interior velocity includes the density current as well as the current associated with horizontal pressure gradients. Expanding Equations (2)-(4) in powers of the Ekman number, $\varepsilon = d / H$, where d is the Ekman depth and H is water depth, we get governing equations for u_i and u_w,

$$\frac{\partial \mathrm{u}_i}{\partial t} + \mathbf{f} \times \mathrm{u}_i = -g\nabla\zeta - \frac{g}{\rho_o}\int_z^0 \rho dz \tag{6}$$

$$\frac{\partial \mathrm{u}_w}{\partial t} + \mathbf{f} \times \mathrm{u}_\mathrm{w} = \frac{\partial}{\partial z}(-\overline{w\mathrm{u}'_w}) \tag{7}$$

where the Reynolds stress is parameterized by a vertical eddy coefficient, A_V,

$$-\overline{w\mathrm{u}'_w} = A_V \frac{\partial \mathrm{u}_w}{\partial z} . \tag{8}$$

The surface boundary condition for the Ekman current is:

$$A_V \left. \frac{\partial \mathrm{u}_w}{\partial z} \right|_{z=0} = \frac{\mathrm{T}_a}{\rho_o} \tag{9}$$

where T_a is wind stress, computed from surface wind fields, U, at 10m height,

$$\mathrm{T}_a = \rho_a C_d |\mathrm{U}|\mathrm{U} , \tag{10}$$

ρ_a is the air density, and C_d, the air-sea drag coefficient. Further details are presented in Perrie et al. (2002).

2.3 Wave-Current Coupling

From Jenkins (1987ab, 1989) and Perrie and Hu (1997), wave modified surface currents are determined by,

$$\frac{\partial \mathrm{u}_E}{\partial t} + \mathbf{f} \times \mathrm{u}_E = \frac{\partial}{\partial z}\left(A_V \frac{\partial \mathrm{u}_E}{\partial z} \right) - \mathbf{f} \times \mathrm{U}_S - 2\pi \int df \int f \mathrm{k} S_{ds}\, 2ke^{2kz}\, d\theta \,. \tag{11}$$

The associated surface boundary conditions, incorporating the effects of the energy input to waves by the wind S_{in},

$$A_V \left. \frac{\partial \mathrm{u}_E}{\partial c} \right|_{c=0} = \frac{\mathrm{T}_a}{\rho_o} - 2\pi \int df \int f \mathrm{k} S_{in}\, d\theta \tag{12}$$

where c is the vertical coordinate z at time $t = 0$. These equations are in terms of the quasi-Eulerian current, u_E, which is the Lagrangian mean current minus the Stokes drift, $\mathrm{u}_L - \mathrm{U}_S$. We can identify the quasi-Eulerian current with the Eulerian-mean current, u_w as long as particle displacements are not so large as to move from one space grid to another, during a given simulation. The second term on the right of (12) is a reduction in the wind stress for current generation, because some goes into wave generation. Stokes drift U_S is the Lagrangian velocity at time t of a particle whose initial position was $(x, y, c, t = 0)$, following Huang (1971),

$$\mathrm{U}_S(\mathrm{x}, t) = 4\pi \iint f \mathrm{k} e^{2kc} E(f, \theta)\, df d\theta \,. \tag{13}$$

2.4 Model Implementation

In the presence of waves the total horizontal current at the surface, u_{surf}, is given by the sum,

$$\mathrm{u}_{surf} = \mathrm{u}_i + \mathrm{u}_E + \mathrm{U}_S \,. \tag{14}$$

The ocean model domain is a rectangle measuring 1200 km X 2240 km with the left side approximately parallel to the Labrador coast, as shown in Figure 1a. Within this domain, the model equations were implemented on a 20 km X 20 km staggered spatial grid (C grid). Seasonal climatological temperature and salinity data from an objective analysis were used to compute the density field (Tang et al., 1999). Six-hourly wind data from Canadian Meteorological Service were used for forcing.

A finite–difference method is used for u_E and Stokes drift U_S, with an implicit time-stepping to satisfy the stability conditions. A grid of 200 points was used in the vertical direction [0, 100] m, varying from 5 mm at the surface to ~1 m at the bottom. The fineness of the grid near the upper surface necessitates a time-step of about 70sec to satisfy the stability condition. The wave model time-step and grid spacing are 1200 sec and 50 km. We used a well-tuned second-generation operational wave model to estimate $E(f, \theta)$ as in Perrie and Hu (1997).

4. CASE STUDY

The storm occurring on 26-27 January is an example of developing synoptic storms that pass across Newfoundland and the Labrador Sea to the Northeast. This storm developed high winds over an extensive region, as it intensified and propagated across the Grand Banks and the Labrador Sea. Winds reached a maximum of almost 25 m/s on 27

January at 00 UTC. Shortly thereafter, winds in the southern Labrador Sea began to significantly weaken while a strong new system pushed across the northern Labrador Sea with associated of high winds.

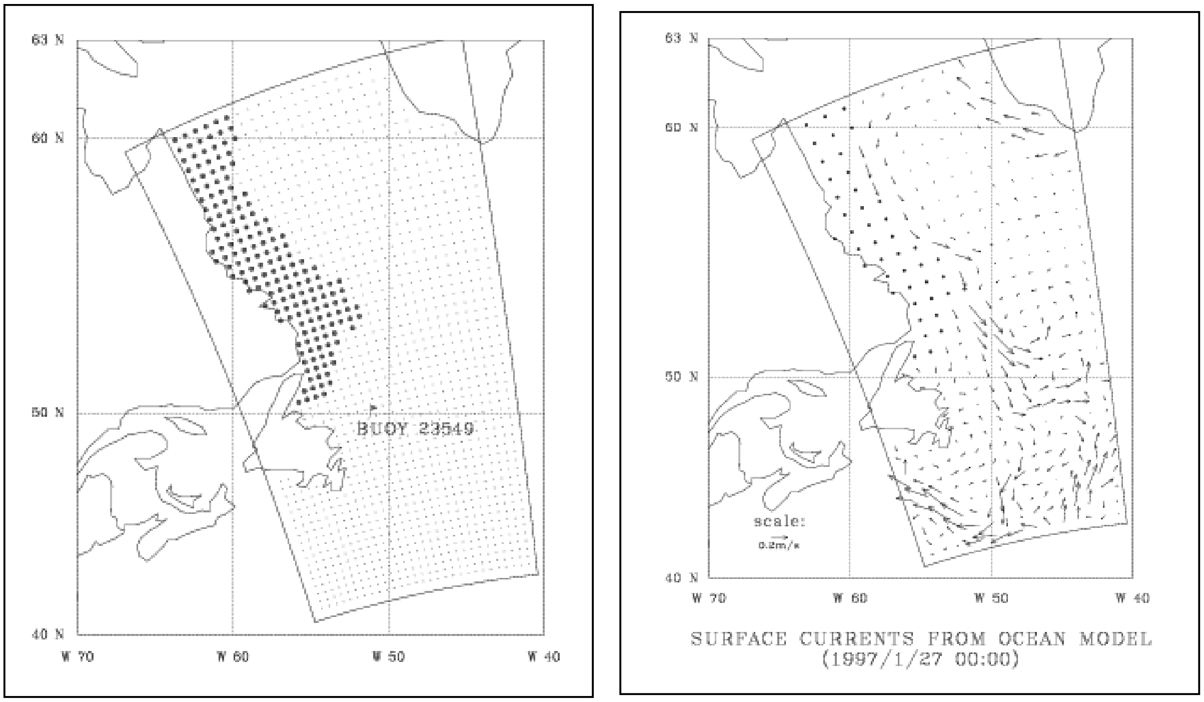

Figure (1a). The ocean model domain (1200 km X 2240 km) with left side parallel to the Labrador coast. Grid spacing is 20 km. The wave model is implemented on the entire map on a 50 km grid. The position of buoy #23549 is indicated. The location of ice cover for the period 26-31 January 1997 is shown (•). (1b) Surface currents from the ocean model, excluding its Ekman layer, for 27 January. This is u_i, with no u_E or U_S.

In Figure 1b, we give the surface current field, u_i, from the ocean model for 27 January 00 UTC, resulting from the density current as well as the current associated with horizontal pressure gradients. This shows the Labrador Current and its extension along the shelf edge of the Labrador Shelf, the N.E. Newfoundland Shelf and the Grand Banks. The corresponding Ekman currents u_w (without waves) for 26-29 January follow the intensification and weakening of the storms as they propagate across the Labrador Sea, driven by winds that increase in magnitude as storms become stronger, and decrease as the storms weaken. These are shown in Figure 2, for the usual Ekman relations Equations (7)-(9). These currents have no explicit consideration of waves. Momentum is passed directly to currents.

As most surface current data are collected with drifters, we will present a comparison with buoy drift data from the LSDCE (Labrador Sea Deep Convection Experiment 1997) campaign, at the Workshop. The buoy (#23549) is shown in Figure 1a. The comparison is for 16-21 December 1996. During the period of the test, wind speeds were reasonably high, often in excess of 10m/s. When winds are low, waves are also low, Ekman currents are small and waves have little effect. We will show (a) the ocean model only, *without* Ekman layer or wave-induced currents, (b) with Ekman layer currents, and (c) with modified Ekman layer currents and wave-induced currents. Thus, it will be shown that the ocean model's estimate for displacement is about 40% of the buoy trajectory, in magnitude. The difference in direction is about 10^o. The Ekman currents gives a combined ocean + Ekman model that is about 80% of the buoy trajectory, and the ocean + wave-modified Ekman currents is almost the same displacement as the buoy drift in this five-day period. Thus, we can show that wave-current interactions have a major effect on surface currents. To cross-link the traditional Ekman layer model which has current u_w to the wave-modified Ekman layer with u_E. We will show the latter as a per centage enhancement on the former for the case study.

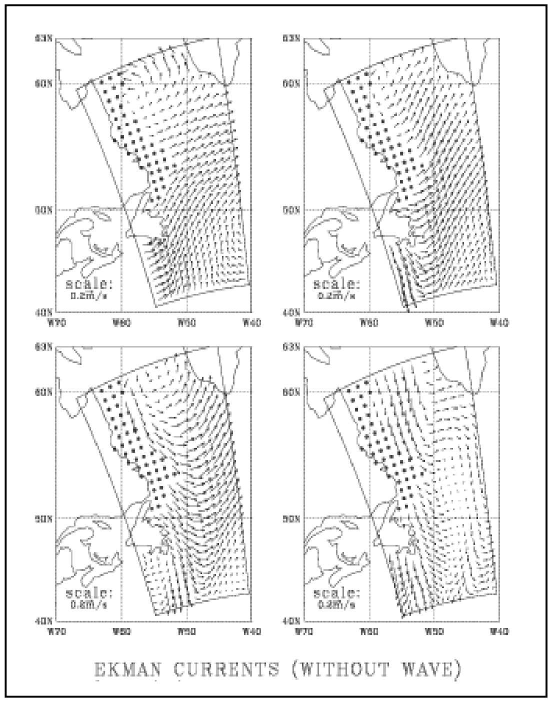

Figure (2). Ekman currents for 27 January at 00, 06, 12, 18 UTC, without wave effects.

5. CONCLUSIONS

The effects of waves on surface currents are considered using a diagnostic ocean model and an operational wave forecasting model. During wave growth, the part of the wind momentum transferred to surface waves through S_{in} exceeds that removed through S_{ds}, and as a result wind stress is less efficient in driving the surface current. When winds and waves are high, wave-induced currents are important even when ocean currents are strong. In rapidly developing storms, wave-modified currents can exceed 40% compared to the total current field, for large ocean regions. Wave-enhanced surface currents evolve as the storms evolve, following the high wind and wave areas. During quiescent periods, wave-induced currents are comparatively weak. The wave effect causes a Stokes drift that can be comparable to the surface currents estimated by the usual Ekman formulation. In terms of total momentum atmosphere-ocean transfers, parameterization of wave-generation causes reductions in the estimated momentum transfer to the ocean due to the wind input to waves, and enhancements due to wave dissipation.

ACKNOWLEDGEMENTS

This study was funded by the Canadian Panel on Energy Research and Development (PERD) of Canada under Projects #534201 on Advanced Wave Models and #21758 on Ocean Surface Currents and Waves. High quality wind fields were provided by CMC (Canadian Meteorological Centre). The drifter data were provided by MEDS, the Marine Environmental Data Service of Canada.

REFERENCES

Hasselmann, S., K. Hasselmann, G.K. Komen, P. Janssen, J.A. Ewing, and V. Cardone, 1988: The WAM model -- a third generation ocean wave prediction model. *J. Phys. Oceanogr.*,**18**, 1775-1810.

Huang, N.E., 1971: Derivation of Stokes drift for a deep-water random gravity wave field. *Deep Sea Res*., **18**, 255-259.

Jenkins, A.D., 1987a: Wind and wave induced currents in a rotating sea with depth varying eddy viscosity. *J. Phys. Oceanogr*., **17**, 938-951.

Jenkins, A.D., 1987b: A Lagrangian model for wind- and wave-induced near-surface currents. *Coastal Engineering*, **11**, 513-526.

Jenkins, A.D., 1989: The use of a wave prediction model for driving a near-surface current model. *Dt. Hydrogr. Z*., **42**, H. 3-6., pages 134-149.

Komen, G.J, L. Cavaleri, M. Donelan, K. Hasselmann, S. Hasselmann and P.A.E.M. Janssen, 1994: Dynamics and Modelling of Ocean Waves, Cambridge University Press, 532 pp.

Perrie, W., and Y. Hu, 1997: Air-ice-ocean momentum exchange, Part II: Ice drift. *J. Phys. Oceanogr.*, **27**, 1976-1996.

Perrie, W., C. Tang, Y. Hu and B. DeYoung, 2002: The impact of waves on surface currents. Submitted to *J. Phys. Oceanogr.*

Tang, C.L. and Q. Gui, 1996: A dynamical model for wind-driven ice motion: application to ice drift on the Labrador Shelf. *Journal of Geophysical Research*, **101**, 28,343 -28,364.

Tang, C.L., Q. Gui and B.M. DeTracey, 1999: A modeling study of upper ocean winter processes. *J. Geophys. Res*., **104**, 23,411-23,425.